The International Journal of Advanced Manufacturing Technology (2019) 100:435–443
https://doi.org/10.1007/s00170-018-2682-6

ORIGINAL ARTICLE

Significance of tool offset and copper interlayer during friction stir welding of aluminum to titanium

Amlan Kar[1] · Satyam Suwas[2] · Satish V. Kailas[1]

Received: 22 January 2018 / Accepted: 10 September 2018 / Published online: 25 September 2018

Abstract

This investigation highlights the influence of tool offset on the microstructural evolution, phase formation, and hardness distribution during friction stir welding (FSW) of commercially pure aluminum (Al) to commercially pure titanium (Ti) with a copper (Cu) interlayer (200-μm thick). It was observed that tool offset position controls the mechanical mixing of materials in the weld nugget. The mechanical mixing also depends on the deformation, fragmentation, and distribution of each material in the weld nugget. The fragmentation of materials leads to the development of comparatively fine particles with variation in size and morphology. Insufficient mixing at higher tool offsets promotes the formation of root defects and produces inferior welds. On the other hand, when the tool offset is less than the optimum value, severe deformation and mechanical mixing lead to the formation of wormhole defects and evolution of intermetallic compounds in the weld. The spatial distribution of particles and intermetallics in the weld nugget leads to a large scatter in hardness values. Since mechanical mixing affects the morphology, phase evolution, and mechanical properties of the weld, tool offset is considered to be a very important parameter to be optimized for monitoring mechanical mixing and further development of the dissimilar weld with interlayer material.

Keywords Tool offset position · Copper interlayer · Mechanical mixing · Defect formation · Intermetallic compound · Hardness distribution

1 Introduction

Aluminum (Al) and titanium (Ti) possess very good complimentary properties like acceptable strength, ductility, low cost, good corrosion resistance, and high toughness. With progress in industrial designs, a hybrid structure made of Al and Ti is likely to be used in many applications in vehicle and aerospace industries. Conventional fusion welding of Al to Ti poses several difficulties such as formation of intermetallic phases [1, 2], distortion and porosity [3], and increase in crack sensitivity [4] in the weld. Here, the weld exhibits inferior mechanical properties primarily due to the evolution of intermetallic compounds [5–7] and defect-free interface [8, 9].

To mitigate the formation of intermetallics, several solid-state welding methods, such as friction welding [10–12], diffusion bonding [13, 14], and friction stir welding [15, 16] were attempted to weld Al and Ti together. Fuji [12] studied the growth of intermetallics during friction welding of pure aluminum and pure titanium. The authors predicted the growth behavior using conventional growth kinetics. Kim et al. [11] showed that the dominant factor in determining the characteristics of Al-Ti weld in friction welding was the thickness of the intermetallic layer. The critical thickness for the best weld properties was measured as 5 μm. Widen et al. [13] studied the mechanical properties of Al/Ti diffusion bond and showed that the joint could be used for high temperature applications. In addition to friction welding and diffusion bonding, fusion welding techniques such as electron beam welding and laser beam welding [6] were attempted to join Al with Ti in the presence of a shielding gas.

Among these joining techniques, a novel solid-state welding technology, namely friction stir welding (FSW), was originally developed for joining difficult-to-join Al alloys [17–20], such as AA7075 [21, 22], and result in better joint

✉ Amlan Kar
amlankar@iisc.ac.in

[1] Department of Mechanical Engineering, Indian Institute of Science, Bengaluru 560012, India

[2] Department of Materials Engineering, Indian Institute of Science, Bengaluru 560012, India

properties than those obtained by fusion techniques in these alloys [17, 23]. In addition, it has also potential to be used in joining of several other structural materials such as Mg alloys [24–26], Cu alloys [27, 28], dissimilar alloys [29], and even pure lead [30]. Friction stir welding has also been applied to several bi-metallic hybrid combinations. FSW was introduced to weld Al to Ti in the recent past [5, 8, 31–35]. The welding efficiency (by FSW) of a joint Al alloy and Ti alloy was reported, with a joint strength of as high as 73% of the base material [8]; and a thin intermetallic layer was identified at the interface. The thickness of the intermetallic compound and corresponding mechanical properties of the weld depend on processing parameters. The important processing parameters in dissimilar FSW are tool offset position [36], tool rotation speed (rpm), welding speed, and position of plates with respect to tool movement and differences in their physical properties. These parameters affect the relative deformation and material flow in the weld nugget, which influence the final properties of the weld. These parameters need to be optimized to obtain a superior weld quality [31, 33, 37]. Furthermore, Chen [5] reported the evolution of Al_3Ti at different welding condition during FSW of Al to Ti. The formation of Al_3Ti is inevitable in Al/Ti welding. The presence of this phase in the weld is detrimental as it leads to crack formation and catastrophic failure of the weld since Al_3Ti is a brittle phase. The formation of Al_3Ti can be reduced by controlling the welding temperature and inserting an interlayer material in dissimilar welding. Dixit et al. [38] showed the importance of choosing a suitable interlayer material in controlling torque, welding temperature, and frictional condition in friction stir welding of aluminum. In their study, it was shown that the presence of insert materials that has lower melting temperature than the FSW processing temperature will melt. This led to a higher processing load and torque and lower welding temperature. Therefore, it is important to find a condition to mitigate the formation of Al_3Ti by optimizing processing parameters and addition of a suitable interlayer material that effectively produce solid solution and/or reduces the formation of brittle intermetallic compounds. In this regards, Kar et al. [39] highlighted the microstructural evolution and mechanical properties of the friction stir welding (FSW) of aluminum (Al) to titanium (Ti) using a nickel (Ni) interlayer at a fixed processing parameter. It was proposed from their study that Ti and Ni were subjected to severe deformation leading to the formation of fine particles that vary in size and shape. At the interfaces of these particles, diffusion and chemical reaction take place, which led to the formation of interlayer and intermetallic compounds. These particles were consolidated in Al that is dynamically recrystallized and hence weld nugget showed a composite characteristic. The particles containing intermetallic compounds acted as a dispersoid in Al matrix leading to substantial enhancement in tensile properties of the weld [15].

Copper (Cu) produces a solid solution as well as an intermetallic compound (Al_2Cu) while reacting with Al. An Al composite containing Al_2Cu phase exhibits less brittleness compared to an Al composite containing Al_3Ti [8, 40, 41]. Furthermore, Cu has a higher solid solubility in Al than in Ti at the welding temperature expected during FSW (~ 450 °C). It was also observed that Al_aCu_b and Cu_cTi_d intermetallic compounds exhibit lower hardness than Al_xTi_y intermetallic compounds [42, 43]. Hence Al_aCu_b and Cu_cTi_d compounds are less brittle than Al_xTi_y intermetallics in the weld. In addition, the melting temperature of Cu (1048 °C) is more than that of Al (660 °C) but less than that of Ti (1670 °C). Therefore, as per the rule of mixture, it is expected that copper would improve the quality of Al/Ti weld in terms of phase evolution and mechanical properties. However, the evolution of intermetallic compounds depends on local composition, which varies with the tool offset position due to variation in the degree of material mixing.

Although there are a few studies about effect of tool offset on binary system [44] such as friction stir welding of Al to Ti [45] and about effect of interlayer on material flow, defect formation, and mechanical properties of the weld [45–47], the influence of tool offset on ternary system such as dissimilar friction stir welding with interlayer has not been explored extensively. In addition, ternary material mixing (mechanical mixing) and mechanisms associated with defect formation and phase formation have not been studied.

The objective of the present investigation is to study the effect of tool offset and copper interlayer on microstructural evolution, phase formation, and mechanical properties during FSW of Al to Ti with a Cu interlayer. To examine the effect of copper, the tool offset position was chosen to vary linearly to optimize mechanical mixing and local composition in the weld to obtain optimum weld properties. Detailed investigations on mechanisms associated with weld formation, phase evolution, and variation in hardness values across the weld cross section were performed at different tool offset positions to find out the effect of Cu mixing in the weld nugget during FSW of Al to Ti.

2 Experimental method

Rolled plates (4-mm thick) of commercially pure aluminum (CP-Al) and commercially pure Titanium (CP-Ti) were chosen as the working materials. The chemical composition (weight %) of these materials is presented in Table 1.

The Ti and Al were fixed on the advancing side (AS) and retreating side (RS) of the tool, respectively. A copper strip of 0.2-mm thickness was used as an interlayer between the Al and Ti plates. The plates were subjected to FSW in a butt-joint configuration using a custom-built 5-axis FSW machine (developed with the help of the Indian Institute of Science

Table 1 Chemical composition (weight %) of the as-received materials used in friction stir butt welding of Al and Ti

	Cu	Mg	Si	Fe	Mn	Ti	Zn	C	Al	Other
CP-Al	0.002	0.003	0.170	0.120	0.002	0.009	0.003		99.661	0.030
CP-Ti				0.300		99.510		0.080		0.110

Bangalore and Bangalore Intregrated System Solution (P) Ltd., Bangalore, India). The details of the machine are tabulated in Table 2. The machine has a capability to vary tool rotational speed, tool traverse speed, and plunge depth (normal load) during an experiment and the same can be used to study the effect of various process parameters during FSW. Since the experimental parameters can be varied during an experiment, the optimization process can be completed with minimum number of experiments using a bottom-up approach [48]. The welding was carried out along the direction perpendicular to rolling direction of the sheet. A cylindrical tool made of WC-8% Co alloy, with shoulder diameter of 18 mm and tool pin diameter of 5.0 mm, was used for welding. The length of the tool pin was 3.2 mm. The process parameters used during FSW were tool rotation speed of 800 rpm, traverse speed of 90 mm/min, and plunge depth of 3.5 mm. The welding was performed by continuously varying the tool offset position from 2.5 to 1.5 mm on the Al side of the faying interface, as schematically illustrated in Fig. 1. Therefore, severe deformation of the processed materials primarily occurs on the aluminum side of the faying interface. This was done to avoid erosion of the tool pin as the flow stress of Ti is much higher than that of Al.

To examine microstructure of the weld, the weld plate was sectioned by electro-discharge machining (EDM) perpendicular to the welding direction. The samples were polished by standard metallographic methods followed by etching with Kroll's reagent for titanium and Keller's reagent for aluminum. The polished and etched samples were examined by an optical microscope (OM) as well as a scanning electron microscope (SEM) equipped with an energy-dispersive spectrometer (EDS). The characterization of phases formed during welding was performed using X-ray diffraction (XRD) method.

Table 2 Details of five-axis friction stir welding machine at the Surface Interaction and Manufacturing Lab IISc, Bengaluru

Number of axis	5-axis simultaneous control
Specimen mounting area	500 mm × 500 mm
Cooling system	Water cooling system
Stroke length	500 mm in the direction of *x*- and *y*-axis
Maximum speed	3000 rpm (revolution per minutes)
Voltage	400 V
Frequency	60 HZ
Position resolution in space	5 μm
Actuators	Low friction actuators with optional hydro-static bearings
Maximum load	50 kN
Maximum rotational speed	3000 rpm

The Vickers hardness measurements of the metallographic specimens (with different tool offsets) across the joint interface were performed at mid-thickness using a Vickers indenter, applying a 200-g load for 10 s. The distance between two adjacent indentations was maintained as 1.0 mm.

3 Results and discussion

3.1 Effect of tool offset on weld morphology

Figure 2 shows optical micrographs of the weld at different tool offsets of 2.5 mm, 2.1 mm, and 1.7 mm. The elemental Al, Ti, and Cu are marked in the figure. The variation in mechanical mixing of the three materials at different tool offset positions is clearly seen in the weld nugget. The elemental Cu is clearly visible at the faying interface at a tool offset of 2.5 mm (Fig. 2a) and the deformation zone is seen only on the Al side of the weld. Two zones are noticed in the weld: they can be demarcated as tool-pin assisted (TPAZ: white dotted zone in Fig. 2) and tool-shoulder-assisted deformation zones (TSAZ: red dotted zone in Fig. 2). The tool pin-assisted deformation zone is visible at the bottom of the weld, whereas the tool-shoulder-assisted deformation zone is observed at the top of the weld. Figure 2b shows the micrograph of the weld at a tool offset of 2.1 mm. In this case, a high fraction of mechanical mixing is noticed when compared to the weld with a 2.5-mm tool offset. No undeformed Cu is noticed at the faying interface, but fine elemental Cu is seen in the mechanically mixed zone of the weld nugget. Interestingly, the shoulder-assisted deformation zone is substantially reduced, with a concomitant increase in the tool-pin assisted deformation zone, when compared to the weld with a 2.5-mm tool offset. Figure 2c shows the micrograph of the weld at a tool offset of 1.7 mm. This weld shows the much higher degree of mechanical mixing and a further increase in the tool-pin assisted deformation zone when compared to the other two welds. Furthermore, based on the color contrast of the optical micrograph, the mechanically mixed zone contains a lower fraction of elemental Cu. Apart from this, a wormhole defect is noticed at the bottom of the weld adjacent to joining interface.

The deformation of materials and consequent mechanical mixing depends on the tool offset position and dimension of the tool pin. The tool interacts with Ti as well as the Cu

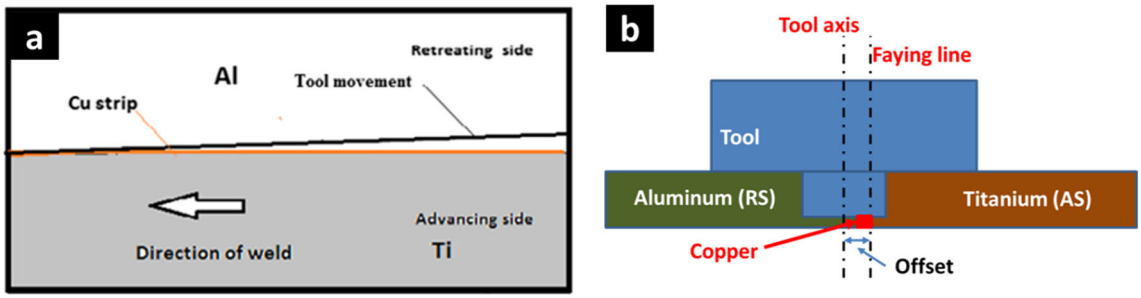

Fig. 1 Schematic diagram of experimental set-up from top side (**a**) and cross section (**b**) of the weld. Ti and Al are clamped in advancing and retreating side of the tool, respectively. Tool offset position changes from 2.5 to 1.0 mm towards Al side from the faying interface

interlayer when tool offset is less than the radius of the tool pin (2.5 mm). Therefore, the minimum and maximum mechanical mixing in the weld nugget are noticed in welds with 2.5 mm and 1.7 mm tool offsets, respectively. The presence of Cu interlayer at the faying interface of the weld with 2.5-mm tool offset is attributed to the minimal interaction and deformation of tool pin with Cu. Insufficient deformation at the faying interface could lead to incomplete welding. On the other hand, a high fraction of Ti and a widespread zone of mechanical mixing in the weld nugget with 1.7-mm tool offset indicate severe interaction and deformation. Extensive mixing of titanium and copper in the weld nugget is seen when at 1.7-mm tool offset. This mixing of the much harder titanium particles in the weld nugget would lead to making the flow of material difficult in this region (Fig. 2c). It produces an inhomogeneous material distribution and chaotic flow in the weld nugget. The presence of hard titanium particles in the weld nugget would make flow of the softer aluminum more difficult. When a harder particle flows in a softer matrix flow, separation is expected at the trailing region of such hard particles. This flow separation would lead to void formation in the weld nugget. Many such voids, indicated by arrows, are shown in Fig. 2c. As the titanium particles restrict the flow in the weld nugget, the material is not able to forge against the advancing side leading to the formation of a wormhole (Fig. 2c). The weld with a 2.1-mm tool offset is subjected to moderate mixing and deformation and hence, does not contain the defects observed in the other welds.

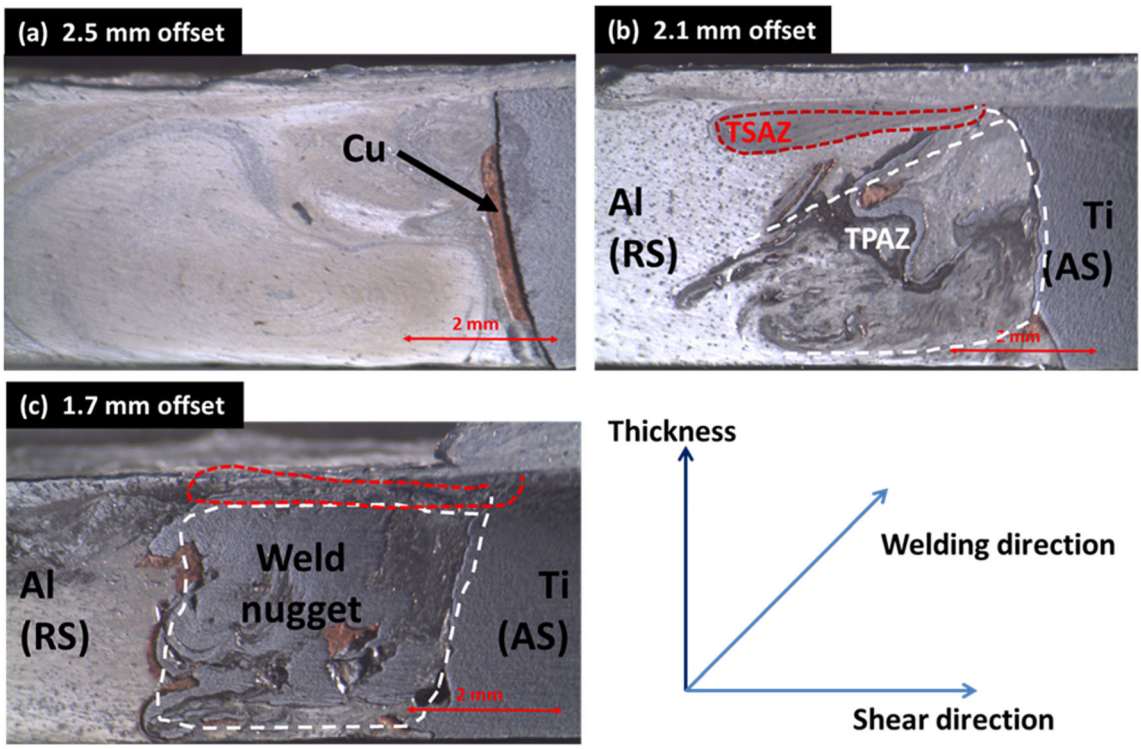

Fig. 2 Optical micrographs of the welds at tool offset of 2.5 mm (**a**), 2.1 mm (**b**), and 1.7 mm (**c**) showing variation in mechanical mixing and deformation of each material

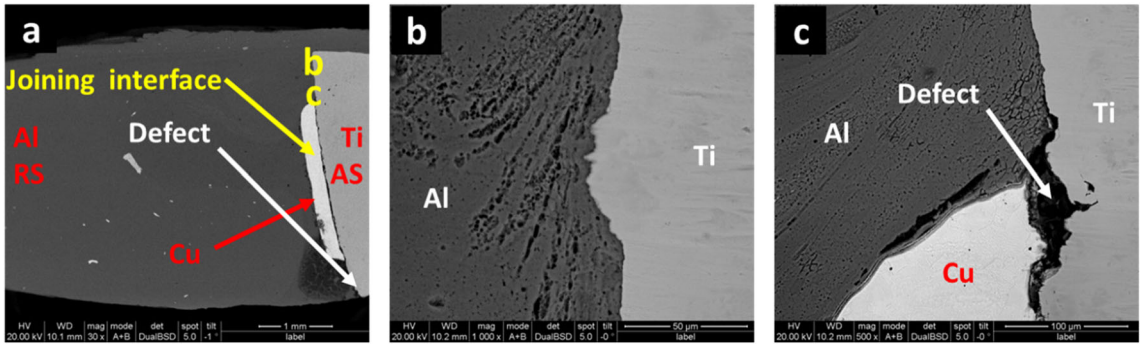

Fig. 3 Scanning electron micrographs of the weld corresponding to 2.5 mm tool offset showing low magnification micrograph (**a**), joining interface (**b**), and a defective zone (**c**) adjacent to the copper interlayer

3.2 Effect of tool offset on microstructure evolution

Figure 3a shows a low magnification microstructure of the weld with a 2.5-mm tool offset through back-scattered electron (BSE) scanning electron microscopy (SEM). The Image contrast in the image demarcates Al, Ti, and Cu, as indicated in the figure. The weld nugget contains Al, Ti, and Cu interlayers. Interestingly, no deformation occurs in Ti at the joining interface. However, a small fraction of Cu interlayer at the top of the weld is subjected to deformation leading to fragmentation into fine Cu particles that are distributed in the weld nugget. Figure 3b exhibits the joint interface from the location indicated in Fig. 3a. No intermediate layer is developed at the interface. However, a wormhole defect is noticed at the joining interface adjacent to Cu interlayer (Fig. 3c).

The detailed interfacial features corresponding to the weld with a 2.1-mm tool offset were examined through SEM. Figure 4a shows the micrograph of the weld cross section containing particles of Ti, Cu (with variation in sizes), and Al matrices. A high fraction of elongated Cu particles is seen. These particles form a mechanically mixed zone (MMZ) in the weld nugget. Figure 4b displays an intermediate layer at the joint interface; the location of the layer is indicated in Fig. 4a. The contrast in the image reveals the formation of intercalated particles and mechanical mixing of Al and Ti. A different type of mechanical mixing is noticed in the weld nugget, as seen in Fig. 4c. The image shows a number of particles with variation in interlayer thickness at the interfaces surrounding the particles. It is also seen that particles of different sizes are mixed with the Al matrix.

Figure 5a shows SEM images from the weld with a 1.7-mm tool offset. It illustrates severe mixing and deformation of the materials. A number of defects are noticed in the weld nugget, as shown in Fig. 5b. These defects are primarily noticed at the interfaces of two MMZs (Fig. 5b, c). The weld also contains particles of different sizes. A careful observation reveals that, unlike smaller particles, defects primarily appear adjacent to large and elongated particles. The Cu particles seen in the weld nugget are comparatively finer compared to Ti particles.

The formation of defects in the weld nugget depends on processing parameters. The weld with a 2.5-mm tool offset shows root defects due to insufficient interaction and deformation of Ti with the tool pin. With reduction in tool offset, the tool pin gradually comes in contact with the Ti interface as well as Cu interface during welding. Such interactions increase with reduction in the tool offset. The interaction of materials leads to the formation of MMZs in the weld nugget and intermediate layers at the joining interfaces. The formation of controlled intermediate layers depends on an optimum tool offset position, which influences mechanical mixing. Severe mechanical mixing could lead to the formation of

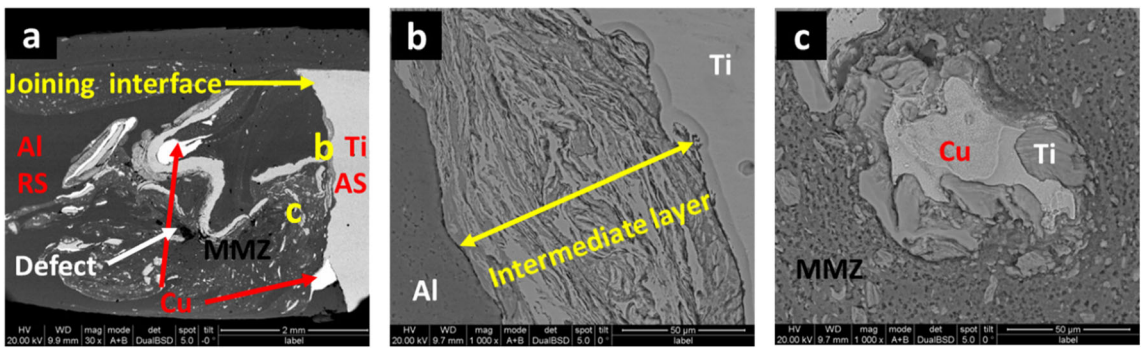

Fig. 4 Scanning electron micrographs of the weld corresponding to 2.1-mm tool offset showing low magnification micrograph (**a**), joining interface with the intermediate layer (**b**), and a mechanically mixed zone (MMZ) (**c**)

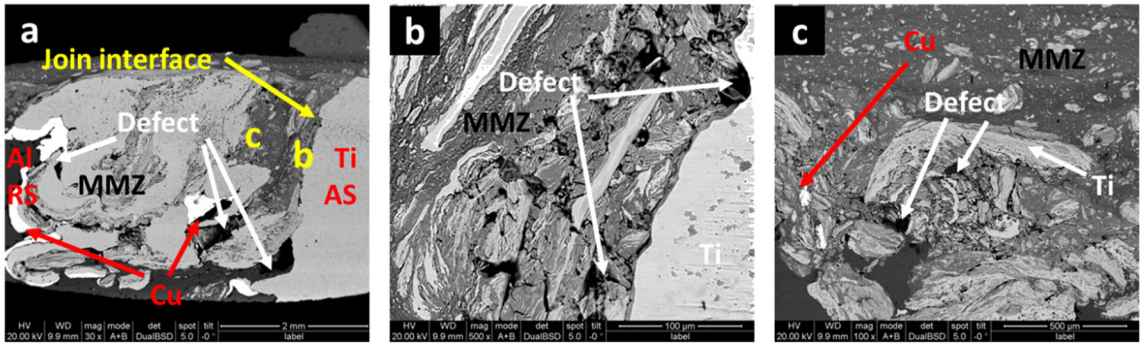

Fig. 5 Scanning electron micrographs of the weld corresponding to 1.7-mm tool offset showing low magnification micrograph (**a**), joining interface with defects (**b**), and a mechanically mixed zone (MMZ) (**c**)

defects when the tool offset is less than the optimum. At the optimum tool offset (2.1 mm offset), flow separation is minimized leading to the filing up of defective zones; hence, a weld with no or minimum defects is expected.

3.3 Effect of tool offset on phase evolution

Figure 6 exhibits XRD patterns from the weld at different tool offset positions. The joint interface was positioned at the center of the exposed area of the XRD beam to identify phase evolution at the center of the welds. The patterns indicate presence of the intermetallic compound Al_3Ti in the weld with a 1.7-mm tool offset. The welds with tool offsets more than 1.7 mm do not contain substantial intermetallic compounds. The evolution of intermetallic compounds is attributed to a high fraction of mechanical mixing and subsequent thermal diffusion at the welding temperature.

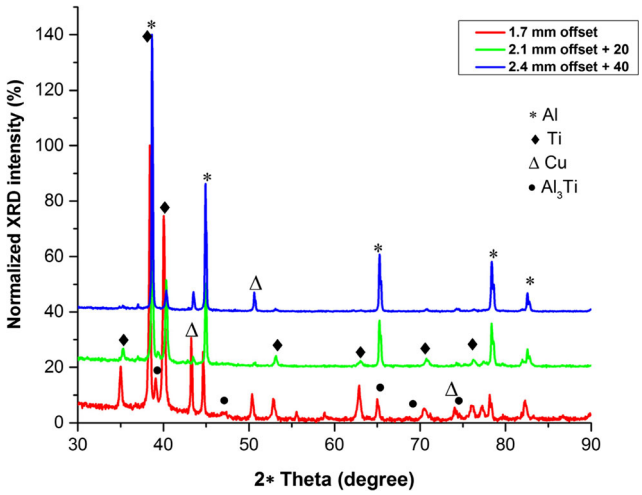

Fig. 6 Normalized X-ray diffraction patterns of the welds at three offset positions showing the evolution of intermetallic phase Al_3Ti and indicating variation in phase evolution at different tool offset position. Formation of phases depends on mechanical mixing that varies with tool offset position

The moderate mixing in the weld with a 2.1-mm tool offset produces less intermetallic compounds compared to the weld with a 1.7-mm tool offset. Optimum deformation and corresponding temperature evolution restrict the evolution intermetallics and formation of defects. The use of copper as an interlayer material leads to lesser amount of the brittle intermetallic compound (Al_3Ti) than the same in the case of direct Al/Ti welds, due to screening of Al with Ti. Time and temperature of welding are the two important factors for the growth of intermetallic compounds at the Al/Ti interface. In gas arc welding [2] and laser welding [49, 50] of Al to Ti, the thickness and morphology of Al_3Ti depend on heat input. However, in the case of solid-state bonding such as diffusion bonding [51], ultrasonic welding [52, 53], and friction stir welding, temperature rises due to the process itself and welding time during welding decides the thickness of intermetallic compounds and properties of the weld. However, it has been noticed that irrespective of welding and joining method, the Al/Ti interface is prone to formation of Al_3Ti [3, 53, 54]. A variation in the evolution of intermetallic compounds was reported by Shouzheng et al. [4] during gas tungsten arc welding of Ti/Al joint by adopting a pulsed current. Such variation was correlated with variation in melting characteristics of the materials to be welded. Rajakumar et al. [51] showed that bonding temperature, bonding pressure, and holding time play a major role to determine the thickness of intermetallic compounds and joint properties. The authors found that the bonds fabricated with the bonding temperature of 510 °C, bonding pressure of 17 MPa, and holding time of 37 min yielded maximum shear strength of 87 MPa, hardness of 163 HV, and interface layer thickness of 7 μm, respectively. In additional to the thickness of the intermetallics, the morphology and their distribution could have an immense influence on properties of the weld. The stirring action and low temperature rise therefore make the FSW attractive for better joint quality.

During FSW, temperature of the weld is expected to be approximately 450 °C. At this temperature, the Al–Cu phase diagram indicates that there are five equilibrium phases, namely Al_2Cu, AlCu, Al_3Cu_4, Al_2Cu_3, and Al_4Cu_9. Wei

Table 3 The Gibbs free energy changes of formations (ΔG) for Al2Cu and Al3Ti at 450 °C (723 K)

Compound	T (°C)	T (K)	ΔG (J/mol)	ΔG at 450 °C (J/mol)
Al_2Cu	450	723	− 15,826.2 + 2.3 × T [55]	− 14,163.3
Al_3Ti	450	723	40,349.6 + 10.36525 × T [56]	− 32,855.5

et al. [55] used the effective Gibbs free energy change of formation model to predict the formation of Al–Cu compounds in Al–Cu joint produced by continuous drive friction welding. The calculation showed that Al_2Cu (Al side) and Al_4Cu_9 (Cu side) appeared first among all the intermetallic compounds. Similarly, the binary Al-Ti phase diagram shows the evolution of several intermetallic compounds, namely $AlTi_3$, AlTi, Al_2Ti, and Al_3Ti at this temperature. The Gibbs free energy for the Al-Ti intermetallics indicates that only Al_3Ti will form at temperatures lower than 500 °C as it has the least free energy. The Gibbs free energy of formation (ΔG) for the possible intermetallics calculated at 450 °C (723 K) is shown in Table 3. Based on the above calculation, the formation of other phases is ruled out.

3.4 Effect of tool offset on hardness

The hardness of the welds with different tool offsets was evaluated by a Vickers hardness tester across the weld cross section at locations of 1.0 mm, 1.5 mm, and 2.5 mm from the weld surface. The hardness of Ti and Al was measured as 148 HV and 24 HV, respectively, before producing the weld. Figure 7 shows the variation in hardness across the welds with different tool offset positions. As expected, the hardness across the weld cross section reduces from the Ti side to Al side. A scatter in the hardness is observed in the nugget zone for all the welds. The scatter in hardness value increases with reduction in the tool offset. A scatter as much as 300 HV is also seen in the weld with a 1.7-mm tool offset, which is attributed to the presence of Ti particles and possible intercalated particles containing intermetallics in the weld nugget. It resembles a swirl-like structure as observed by Wei et al. [35, 57].

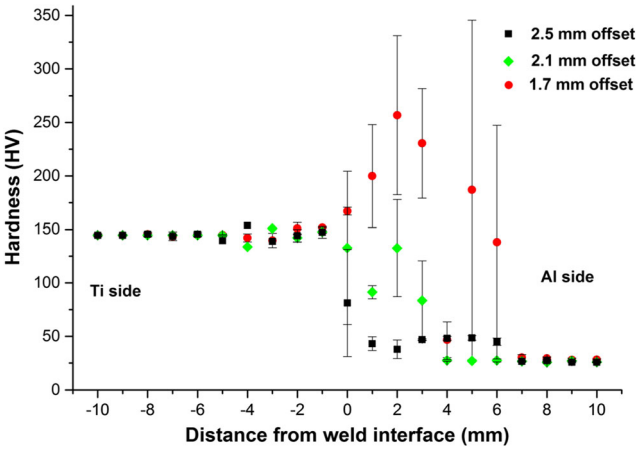

Fig. 7 Variation in hardness distribution across the welds with different tool offset positions. A substantial variation in hardness is noticed for all the welds. However, maximum variation is seen in the weld with 1.7 tool offset due to severe mechanical mixing

4 Conclusion

In the present work, friction stir welding of commercially pure aluminum to commercially pure titanium with a copper interlayer was successfully carried out. The ternary mechanical mixing (which is influenced by tool offset position) and related microstructural evolution and mechanical properties of the weld were investigated in detail. Based on observations, the following conclusions were drawn:

1. The tool offset has an immense influence on the deformation and ternary mechanical mixing of elements in the weld nugget. The mixing depends on the interaction of the tool with the materials. Such interactions increase with reduction in tool offset leading to severe deformation and mechanical mixing.
2. A lower amount of mechanical mixing leads to root defects and hence joining does not take place at the joining interface. On the other hand, intense mechanical mixing promotes the formation of wormhole defects. The formation of such defects is attributed to the chaotic material flow in dissimilar welding, the difference in flow behavior of materials, and flow restriction of Al matrix by particles during welding.
3. The ternary mechanical mixing influences phase evolution in the weld nugget. A high fraction of the intermetallic compound Al_3Ti evolved in the weld with a 1.7-mm tool offset. The high amount of mechanical mixing of copper with Al and Ti creates the local elemental ratio required for the formation of different intermetallic compounds. The elemental diffusion at the welding temperature activates the reaction for evolution of Al_3Ti. The presence of only Al_3Ti is due to its lower free energy of formation among all the compounds that could possibly form at the welding temperature.
4. The distribution of hardness value varies with tool offset. The large scatter in hardness in the weld with a lower tool offset is attributed to severe mechanical mixing and evolution of intermetallic compounds at the interfaces.

5. It is imperative to optimize mechanical mixing in the weld nugget by adjusting the tool offset position. A defect-free weld with fewer fractions of intermetallic compounds is obtained by careful selection of the tool offset. It is thus seen that tool offset is a highly influential parameter for better welds between aluminum and titanium with copper interlayer.

Acknowledgments We would like to thank the Institute X-ray facility and Advanced Facility for Microscopy and Microanalysis (AFMM) at the Indian Institute of Science (IISc), Bangalore, for providing the facilities.

Funding information The authors would like to thank the Defense Research and Development Organization (DRDO), Department of Science and Technology (DST), and Ministry of Human Resources Development (MHRD), India, for the support and research funding.

References

1. Sujata M, Bhargava S, Sangal S (1997) On the formation of TiAl3 during reaction between solid Ti and liquid Al. J Mater Sci Lett 16(13):1175–1178. https://doi.org/10.1023/a:1018509026596
2. Shouzheng W, Yajiang L, Juan W, Kun L, Pengfei Z (2014) Microstructure and joining mechanism of Ti/Al dissimilar joint by pulsed gas metal arc welding. Int J Adv Manuf Technol 70(5): 1137–1142. https://doi.org/10.1007/s00170-013-5290-5
3. Chen Y, Chen S, Li L (2008) Effects of heat input on microstructure and mechanical property of Al/Ti joints by rectangular spot laser welding-brazing method. Int J Adv Manuf Technol 44(3):265–272. https://doi.org/10.1007/s00170-008-1837-2
4. Shouzheng W, Yajiang L, Juan W, Kun L (2014) Improving of interfacial microstructure of Ti/Al joint during GTA welding by adopting pulsed current. Int J Adv Manuf Technol 73(9):1307–1312. https://doi.org/10.1007/s00170-014-5929-x
5. Chen YC, Nakata K (2009) Microstructural characterization and mechanical properties in friction stir welding of aluminum and titanium dissimilar alloys. Mater Des 30(3):469–474. https://doi.org/10.1016/j.matdes.2008.06.008
6. Kreimeyer M, Wagner F, Vollertsen F (2005) Laser processing of aluminum–titanium-tailored blanks. Opt Lasers Eng 43(9):1021–1035. https://doi.org/10.1016/j.optlaseng.2004.07.005
7. Majumdar B, Galun R, Weisheit A, Mordike BL (1997) Formation of a crack-free joint between Ti alloy and Al alloy by using a high-power CO2 laser. J Mater Sci 32(23):6191–6200. https://doi.org/10.1023/a:1018620723793
8. Dressler U, Biallas G, Alfaro Mercado U (2009) Friction stir welding of titanium alloy TiAl6V4 to aluminium alloy AA2024-T3. Mater Sci Eng A 526(1–2):113–117. https://doi.org/10.1016/j.msea.2009.07.006
9. Watanabe T, Takayama H, Yanagisawa A (2006) Joining of aluminum alloy to steel by friction stir welding. J Mater Process Technol 178(1):342–349. https://doi.org/10.1016/j.jmatprotec.2006.04.117
10. Fuji A (2002) In situ observation of interlayer growth during heat treatment of friction weld joint between pure titanium and pure aluminium. Sci Technol Weld Join 7(6):413–416. https://doi.org/10.1179/136217102225006903
11. Kim YC, Fuji A (2002) Factors dominating joint characteristics in Ti – Al friction welds. Sci Technol Weld Join 7(3):149–154. https://doi.org/10.1179/136217102225004185
12. Fuji A, Ikeuchi K, Sato YS, Kokawa H (2004) Interlayer growth at interfaces of Ti/Al–1%Mn, Ti/Al–4·6%Mg and Ti/pure Al friction weld joints by post-weld heat treatment. Sci Technol Weld Join 9(6):507–512. https://doi.org/10.1179/136217104225021797
13. Wilden J, Bergmann JP (2004) Manufacturing of titanium/aluminium and titanium/steel joints by means of diffusion welding. Weld Cut 56(5):285–290
14. Çam G, Koçak M, Dobi D, Heikinheimo L, Siren M (1997) Fracture behaviour of diffusion bonded bimaterial Ti–Al joints. Sci Technol Weld Join 2(3):95–101. https://doi.org/10.1179/stw.1997.2.3.95
15. Kar A, Suwas S, Kailas SV (2018) Two-pass friction stir welding of aluminum alloy to titanium alloy: a simultaneous improvement in mechanical properties. Mater Sci Eng A 733:199–210. https://doi.org/10.1016/j.msea.2018.07.057
16. Kar A, Devinder Y, Suwas S, Kailas SV (2016) A study of deformation and microstructural evolution in friction stir welding of aluminum and titanium. Trends Weld Res S39-1:728–731
17. Çam G, İpekoğlu G (2017) Recent developments in joining of aluminum alloys. Int J Adv Manuf Technol 91(5):1851–1866. https://doi.org/10.1007/s00170-016-9861-0
18. Çam G, Mistikoglu S (2014) Recent developments in friction stir welding of Al-alloys. J Mater Eng Perform 23(6):1936–1953. https://doi.org/10.1007/s11665-014-0968-x
19. Bozkurt Y, Salman S, Çam G (2013) Effect of welding parameters on lap shear tensile properties of dissimilar friction stir spot welded AA 5754-H22/2024-T3 joints. Sci Technol Weld Join 18(4):337–345. https://doi.org/10.1179/1362171813y.0000000111
20. Zhang HJ, Wang M, Qi RL, Zhu Z, Zhang X, Yu T, Wu ZQ (2017) Effect of rotation speed on nugget structure and property of high rotation speed friction stir welded Al-Mn aluminum alloy. Int J Adv Manuf Technol 92(5–8):2401–2410. https://doi.org/10.1007/s00170-017-0295-0
21. İpekoğlu G, Erim S, Çam G (2014) Effects of temper condition and post weld heat treatment on the microstructure and mechanical properties of friction stir butt-welded AA7075 Al alloy plates. Int J Adv Manuf Technol 70(1):201–213. https://doi.org/10.1007/s00170-013-5255-8
22. Mao Y, Ke L, Chen Y, Liu F, Xing L (2017) Improving local and global mechanical properties of friction stir welded thick AA7075-T6 joints by optimizing pin-tip profile. Int J Adv Manuf Technol 88(5–8):1863–1875. https://doi.org/10.1007/s00170-016-8886-8
23. Çam G (2011) Friction stir welded structural materials: beyond Al-alloys. Int Mater Rev 56(1):1–48. https://doi.org/10.1179/095066010x12777205875750
24. Mironov S, Onuma T, Sato YS, Yoneyama S, Kokawa H (2017) Tensile behavior of friction-stir welded AZ31 magnesium alloy. Mater Sci Eng A 679:272–281. https://doi.org/10.1016/j.msea.2016.10.036
25. Buffa G, Campanella D, Forcellese A, Fratini L, La Commare U, Simoncini M (2018) In-process control strategies for friction stir welding of AZ31 sheets with non-uniform thickness. Int J Adv Manuf Technol 95(1–4):493–504. https://doi.org/10.1007/s00170-017-1223-z
26. Dorbane A, Ayoub G, Mansoor B, Hamade RF, Kridli G, Shabadi R, Imad A (2016) Microstructural observations and tensile fracture behavior of FSW twin roll cast AZ31 Mg sheets. Mater Sci Eng A 649:190–200. https://doi.org/10.1016/j.msea.2015.09.097
27. Küçükömeroğlu T, Şentürk E, Kara L, İpekoğlu G, Çam G (2016) Microstructural and mechanical properties of friction stir welded nickel-aluminum bronze (NAB) alloy. J Mater Eng Perform 25(1):320–326. https://doi.org/10.1007/s11665-015-1838-x

28. Çam G, Serindağ HT, Çakan A, Mistikoglu S, Yavuz H (2008) The effect of weld parameters on friction stir welding of brass plates. Mater Werkst 39(6):394–399. https://doi.org/10.1002/mawe.200800314
29. Gao Y, Morisada Y, Fujii H, Liao J (2018) Dissimilar friction stir lap welding of magnesium to aluminum using plasma electrolytic oxidation interlayer. Mater Sci Eng A 711:109–118. https://doi.org/10.1016/j.msea.2017.11.034
30. Günen A, Kanca E, Demir M, Çavdar F, Mistikoğlu S, Çam G (2018) Microstructural and mechanical properties of friction stir welded pure lead. Indian J Eng Mat Sci 25(1):26–32
31. Chen Y-h, Ni Q, Ke L-m (2012) Interface characteristic of friction stir welding lap joints of Ti/Al dissimilar alloys. Trans Nonferrous Metals Soc China 22(2):299–304. https://doi.org/10.1016/S1003-6326(11)61174-6
32. Aonuma M, Nakata K (2011) Dissimilar metal joining of 2024 and 7075 aluminium alloys to titanium alloys by friction stir welding. Mater Trans 52(5):948–952. https://doi.org/10.2320/matertrans.L-MZ201102
33. Bang H, Bang H, Song H, Joo S (2013) Joint properties of dissimilar Al6061-T6 aluminum alloy/Ti–6%Al–4%V titanium alloy by gas tungsten arc welding assisted hybrid friction stir welding. Mater Des 51:544–551. https://doi.org/10.1016/j.matdes.2013.04.057
34. Aonuma M, Nakata K (2010) Effect of calcium on intermetallic compound layer at interface of calcium added magnesium–aluminum alloy and titanium joint by friction stir welding. Mater Sci Eng B 173(1–3):135–138. https://doi.org/10.1016/j.mseb.2009.12.015
35. Wei Y, Li J, Xiong J, Huang F, Zhang F, Raza SH (2012) Joining aluminum to titanium alloy by friction stir lap welding with cutting pin. Mater Charact 71:1–5. https://doi.org/10.1016/j.matchar.2012.05.013
36. Cole EG, Fehrenbacher A, Duffie NA, Zinn MR, Pfefferkorn FE, Ferrier NJ (2014) Weld temperature effects during friction stir welding of dissimilar aluminum alloys 6061-t6 and 7075-t6. Int J Adv Manuf Technol 71(1):643–652. https://doi.org/10.1007/s00170-013-5485-9
37. Rajakumar S, Muralidharan C, Balasubramanian V (2011) Statistical analysis to predict grain size and hardness of the weld nugget of friction-stir-welded AA6061-T6 aluminium alloy joints. Int J Adv Manuf Technol 57(1):151–165. https://doi.org/10.1007/s00170-011-3279-5
38. Dixit S, MH C, Kailas SV, Chattopadhyay K (2017) Role of insert material on process loads during FSW. Int J Adv Manuf Technol 91(9):3427–3435. https://doi.org/10.1007/s00170-016-9974-5
39. Kar A, Suwas S, Kailas SV (2017) An investigation on friction stir welding of aluminum to titanium using a nickel interlayer. Conference proceedings: Indian Institute of Welding-International Congress C051: 261–266
40. Abdollah-Zadeh A, Saeid T, Sazgari B (2008) Microstructural and mechanical properties of friction stir welded aluminum/copper lap joints. J Alloys Compd 460(1):535–538. https://doi.org/10.1016/j.jallcom.2007.06.009
41. Barekatain H, Kazeminezhad M, Kokabi AH (2014) Microstructure and mechanical properties in dissimilar butt friction stir welding of severely plastic deformed aluminum AA 1050 and commercially pure copper sheets. J Mat Sci Technol 30(8):826–834. https://doi.org/10.1016/j.jmst.2013.11.007
42. Kim S-Y, Jung S-B, Shur C-C, Yeon Y-M, Kim D-U (2003) Mechanical properties of copper to titanium joined by friction welding. J Mater Sci 38(6):1281–1287. https://doi.org/10.1023/a:1022890611264
43. Xue P, Xiao BL, Ni DR, Ma ZY (2010) Enhanced mechanical properties of friction stir welded dissimilar Al–Cu joint by intermetallic compounds. Mater Sci Eng A 527(21–22):5723–5727. https://doi.org/10.1016/j.msea.2010.05.061
44. Ouyang JH, Kovacevic R (2002) Material flow and microstructure in the friction stir butt welds of the same and dissimilar aluminum alloys. J Mater Eng Perform 11(1):51–63. https://doi.org/10.1007/s11665-002-0008-0
45. Song Z, Nakata K, Wu A, Liao J, Zhou L (2014) Influence of probe offset distance on interfacial microstructure and mechanical properties of friction stir butt welded joint of Ti6Al4V and A6061 dissimilar alloys. Mater Des 57:269–278. https://doi.org/10.1016/j.matdes.2013.12.040
46. Çam G, İpekoğlu G, Tarık Serindağ H (2014) Effects of use of higher strength interlayer and external cooling on properties of friction stir welded AA6061-T6 joints. Sci Technol Weld Join 19(8):715–720. https://doi.org/10.1179/1362171814y.0000000247
47. Xu RZ, Ni DR, Yang Q, Liu CZ, Ma ZY (2015) Influence of Zn interlayer addition on microstructure and mechanical properties of friction stir welded AZ31 Mg alloy. J Mater Sci 50(12):4160–4173. https://doi.org/10.1007/s10853-015-8841-3
48. Nadammal N, Kailas SV, Suwas S (2015) A bottom-up approach for optimization of friction stir processing parameters; a study on aluminium 2024-T3 alloy. Mat Des (1980–2015) 65:127–138. https://doi.org/10.1016/j.matdes.2014.09.005
49. Chen S, Yang D, Li M, Zhang Y, Huang J, Yang J, Zhao X (2016) Laser penetration welding of an overlap titanium-on-aluminum configuration. Int J Adv Manuf Technol 87(9):3069–3079. https://doi.org/10.1007/s00170-016-8732-z
50. Gao X-L, Liu J, Zhang L-J (2018) Effect of heat input on microstructure and mechanical properties of pulsed laser welded joints in Ti6Al4V/Nb dissimilar alloys. Int J Adv Manuf Technol 94(9):3937–3947. https://doi.org/10.1007/s00170-017-1134-z
51. Rajakumar S, Balasubramanian V (2016) Diffusion bonding of titanium and AA 7075 aluminum alloy dissimilar joints—process modeling and optimization using desirability approach. Int J Adv Manuf Technol 86(1):1095–1112. https://doi.org/10.1007/s00170-015-8223-7
52. Zhu Z, Lee KY, Wang X (2012) Ultrasonic welding of dissimilar metals, AA6061 and Ti6Al4V. Int J Adv Manuf Technol 59(5):569–574. https://doi.org/10.1007/s00170-011-3534-9
53. Zhou L, Min J, He WX, Huang YX, Song XG (2018) Effect of welding time on microstructure and mechanical properties of Al-Ti ultrasonic spot welds. J Manuf Process 33:64–73. https://doi.org/10.1016/j.jmapro.2018.04.013
54. Plaine AH, Suhuddin UFH, Alcântara NG, dos Santos JF (2017) Microstructure and mechanical behavior of friction spot welded AA6181-T4/Ti6Al4V dissimilar joints. Int J Adv Manuf Technol 92(9):3703–3714. https://doi.org/10.1007/s00170-017-0439-2
55. Wei Y, Li J, Xiong J, Zhang F (2016) Investigation of interdiffusion and intermetallic compounds in Al–Cu joint produced by continuous drive friction welding. Eng Sci Technol Int J 19(1):90–95. https://doi.org/10.1016/j.jestch.2015.05.009
56. Kattner UR, Lin J-C, Chang YA (1992) Thermodynamic assessment and calculation of the Ti-Al system. Metall Trans A 23(8):2081–2090. https://doi.org/10.1007/bf02646001
57. Wei Y, Aiping W, Guisheng Z, Jialie R (2008) Formation process of the bonding joint in Ti/Al diffusion bonding. Mater Sci Eng A 480(1–2):456–463. https://doi.org/10.1016/j.msea.2007.07.027